ORIGINAL RESEARCH

Dependability of Automated Breast Ultrasound (ABUS) in Assessing Breast Imaging Reporting and Data System (BI-RADS) Category and Size of Malignant Breast Lesions Compared with Handheld Ultrasound (HHUS) and Mammography (MG)

He Chen[1]
Ming Han[2]
Hui Jing[1]
Zhao Liu [ID][1]
Haitao Shang [ID][1]
Qiucheng Wang[1]
Wen Cheng[1]

[1]Department of Ultrasound, Harbin Medical University Cancer Hospital, Harbin City, Heilongjiang Province, People's Republic of China; [2]Department of General Surgery, Heji Hospital of Changzhi Medical College, Changzhi City, Shanxi Province, People's Republic of China

Correspondence: Wen Cheng;
Qiucheng Wang
Department of Ultrasound, Harbin Medical University Cancer Hospital, No. 150, Haping Road, Nangang District, Harbin City, 150081, Heilongjiang Province, People's Republic of China
Tel +86 13313677182; +86 13836134350
Fax +86 45185718392
Email hrbchengwen@163.com;
haerbincss@126.com

Purpose: This study aimed to evaluate the dependability of automated breast ultrasound (ABUS) compared with handheld ultrasound (HHUS) and mammography (MG) on the Breast Imaging Reporting and Data System (BI-RADS) category and size assessment of malignant breast lesions.

Patients and Methods: A total of 344 confirmed malignant lesions were recruited. All participants underwent MG, HHUS, and ABUS examinations. Agreements on the BI-RADS category were evaluated. Lesion size assessed using the three methods was compared with the size of the pathological result as the control. Regarding the four major molecular subtypes, correlation coefficients between size on imaging and pathology were also evaluated.

Results: The agreement between ABUS and HHUS on the BI-RADS category was 86.63% (kappa = 0.77), whereas it was 32.22% (kappa = 0.10) between ABUS and MG. Imaging lesion size compared to pathologic lesion size was assessed correctly in 36.92%/52.91% (ABUS), 33.14%/48.84% (HHUS) and 33.44%/43.87% (MG), with the threshold of 3 mm/5 mm, respectively. The correlation coefficient of size of ABUS-Pathology (0.75, Spearman) was statistically higher than that of the MG-Pathology (0.58, Spearman) with $P < 0.01$, but not different from that of the HHUS-Pathology (0.74, Spearman) with $P > 0.05$. The correlation coefficient of ABUS-Pathology was statistically higher than that of MG-Pathology in the triple-negative subtype, luminal B subtype, and luminal A subtype ($P<0.01$).

Conclusion: The agreement between ABUS and HHUS in the BI-RADS category was good, whereas that between ABUS and MG was poor. ABUS and HHUS allowed a more accurate assessment of malignant tumor size compared to MG.

Keywords: automated breast ultrasound, hand-held ultrasound, mammography, breast imaging reporting and data system category, size assessment

Introduction

Female breast cancer is the most commonly diagnosed cancer with estimated 2.3 million new cases, which has surpassed lung cancer, and early detection of breast malignant tumors considerably improves clinical treatment outcomes and quality of life.[1] Significant efforts have been made to improve imaging capabilities to detect breast lesions early. Mammography (MG) remains the gold standard for

breast cancer screening, with a sensitivity of 85%.[2] However, the sensitivity of MG screening is limited in women with dense breasts.

The value of handheld ultrasound (HHUS) has been recognized in many prospective studies that indicated that adding HHUS screening to mammography demonstrated an increase in breast cancer detection rates.[3–6] However, its widespread integration into the screening environment is restricted owing to a few drawbacks, such as lack of standardization of technique, time consumption, and a small field of view (FOV).[7,8]

Currently, automated breast ultrasound (ABUS) is an emerging promising technology for breast cancer diagnosis.[9] ABUS provides reproducible, high-resolution images and operator independence using an automated scanner with a large FOV. The European Asymptomatic Screening Study (EASY) showed that adding ABUS to MG screening in women with dense breasts significantly increased breast cancer detection rates.[10] A multi-institutional study on >15,000 asymptomatic women indicated that adding ABUS to digital mammography resulted in an increase in detection of two cancers per 1000 women screened.[11]

Although the use of ultrasonography in breast cancer detection has been established, little is known about whether results regarding the clinical application of ABUS assessments of the BI-RADS category are in concordance with those of HHUS and MG. A precise category of suspicious breast masses offers vital information for the interpretation of biopsy results based on imaging findings. Discordance in BI-RADS category required by the type of imaging method used could extraordinarily affect the quality of patient care, and potentially result in delayed cancer diagnosis or unnecessary surgery. What's more, accurate assessment of lesion size is important for choosing a treatment plan and influencing the curative effect and prognosis. In particular, in breast-conserving surgery, negative resection margins contribute to decreased rates of locoregional recurrence (LRR).[12] Chang et al reported good reproducibility of size measurement, mass localization, and category on serial examinations with ABUS.[9] Nevertheless, few studies have compared the accuracy of size assessment for breast malignancies between ABUS and other current imaging methods.

We aimed to evaluate the dependability of ABUS in comparison to HHUS and MG with respect to the Breast Imaging Reporting and Data System (BI-RADS) category and size assessment of breast malignant lesions.

Materials and Methods
Study Participants
From January 2019 to October 2020, 388 patients with 403 lesions (proven to be malignant by surgical specimen histopathology) were retrospectively reviewed. All patients were examined using ABUS, HHUS, and MG before surgery. To compare lesion size assessed via three methods to the surgical specimen histopathology size, 55 patients with 59 lesions who underwent neoadjuvant chemotherapy were excluded (almost all patients underwent MG only once). Finally, 333 patients (mean age, 53.1 years; age range, 27–77 years) with 344 lesions were included. All images obtained by ABUS, HHUS, and MG were reviewed, and the results of surgical specimen histopathology were recorded.

ABUS
All participants underwent ABUS, HHUS, and MG examinations on the same day preoperatively before surgery. We used Invenia ABUS (Automated Breast Ultrasound System, GE Healthcare, Sunnyvale, CA, USA) for examinations. The scan was performed by two experienced technicians. A sponge was placed under the shoulder to keep the breast flat, with the nipple pointing straight up. Participants were asked not to move, and to breathe as smoothly as possible. The lotion was evenly smeared on the breast, with an additional amount applied around the nipple to fully image the skin in contact with the probe. Each breast was imaged in three basic views: anteroposterior, lateral, and medial, with a 15.3 cm long and automated 6–14 MHz linear array transducer attached to a rigid compression plate. Scanning began from the feet toward the head. Next, the whole breast was reconstructed in the coronal and sagittal planes using approximately 300 2D images from every view. A nipple marker was noted according to each patient's anatomy in each examination to localize the lesions accurately. The average time taken for the examination was approximately 10–15 min.

HHUS
HHUS examinations were performed with a linear transducer at 10–15 MHz grayscale (GE Healthcare LOGIQ E9, Philips EPIQ5, and EPIQ7). Patients were instructed to raise their hands above the head in the supine position. Bilateral breasts, as well as lymph nodes in the armpits and supraclavicular fossae, were included in the scope of the examination. Overlapping scanning was performed in

the mammillo-radial (parallel to ducts) and anti-radial planes with delivery from the nipple to the ambient breast tissue.

MG

MG images were obtained using a GE Senographe DS (GE Medical Systems, Milwaukee, WI, USA), Hologic Selenia (Hologic, Bedford, MA, USA), and Fujifilm FDR MS-2500 (Fujifilm Corp, Tokyo, Japan). Each breast was imaged in the mediolateral oblique (MLO) and craniocaudal (CC) views.

Image Evaluation

Digitally saved images and datasets by MG, HHUS and ABUS were retrospectively analyzed. All of the radiologists were blinded to the results of pathology. The interpreting radiologist for one imaging method was blinded to the results of other types. Mammography was evaluated by two experienced radiologists blinded to each other's results, by using BI-RADS category.[13] All the volumes acquired by ABUS were automatically transferred to a dedicated workstation for interpretation. The workstation processed the dataset in various multiplanar reconstructions. ABUS and HHUS images were interpreted by two breast radiologists with 7 and 10 years of experience, respectively. The following descriptors were used: shape, margin, orientation, echo pattern, posterior features, and calcifications. Images for each lesion obtained with both HHUS and ABUS were also interpreted per American BI-RADS categorization. BI-RADS category >3 was consistent with malignant histological results. Agreements of the BI-RADS categories between ABUS and HHUS, as well as ABUS and MG, were evaluated.

Measurements of lesions detected with ABUS were compared with those obtained using HHUS, MG, and histopathology results. The size of the lesion was defined as the maximum diameter via all methods. For all malignant lesions, the accuracy of the mass size obtained with ABUS, HHUS, and MG compared to histopathology was evaluated. The threshold criterion for the extent of malignant breast tumors varies from 2 to 20 mm with an indefinite reference. We arbitrarily chose values of 3 mm and 5 mm to compare the two different thresholds. For 3 mm as the threshold criterion, we considered size estimates of ±3 mm as accurate estimation, more than +3 mm as overestimation, and less than −3 mm as under-estimation. Subsequently, we changed the threshold to 5 mm

(±5 mm as accurate estimation, more than +5 mm as overestimation, and less than −5 mm as under-estimation).

Histopathology

Pathologic diagnoses and tumor sizes were evaluated. All analyses of images used pathologic results as the gold standard. The tumors were cut into parallel slices along the sagittal plane. Subsequently, the slice showing the largest size of the cut surface was used to measure the longest and vertical diameters of the tumor. In addition, several markers were tested in our study for histopathologic features: estrogen receptor (ER), progesterone receptor (PR), human epidermal growth factor receptor 2 (HER2), and antigen KI67 (Ki-67). In terms of St. Gallen International Expert Consensus 2013 the major four subtypes were classified as follows: (1) the luminal A subtype was "ER and PR positive, HER2 negative, and Ki-67 low (<14%)"; (2) the luminal B subtype was "ER positive, HER2 negative, Ki-67 high (≥14%) or/and, PR negative; ER positive, HER2 enriched or amplified, any Ki-67, and any PR"; (3) the HER2 enriched subtype was "HER2 enriched or amplified, and ER and PR absent"; and (4) the triple negative subtype was "ER and PR absent, and HER2 negative".[14]

Statistical Analysis

Measurement data were described as mean ± standard deviation (SD). Enumeration data are presented as frequency (%) and percentage. ANOVA was used for statistical testing among the three groups. The BI-RADS categories by ABUS, HHUS, and MG were cross-tabulated. With regard to the agreement between ABUS, HHUS, and MG, the kappa statistic was estimated. Spearman correlation coefficients were calculated to analyze and compare the association between the measurements made using the three imaging methods and the histopathological determination of the four major molecular subtypes. Paired-sample U-tests were performed to analyze the significance of differences in correlation coefficients.

Results

This study analyzed 344 histologically confirmed malignant lesions of 333 patients who underwent ABUS, HHUS, and MG examinations followed by surgery. Histopathologic analysis revealed 166 luminal A subtypes (48.26%), 116 luminal B subtypes (33.72%), 30 triple-negative subtypes (8.72%), and 32 HER2-enriched subtypes (9.30%).

BI-RADS Category in Three Imaging Methods

Both ABUS and HHUS detected 344 lesions belonging to BI-RADS 3, 4, or 5. MG assessed 330 cases belonging to BI-RADS 3, 4, or 5, and 14 cases belonging to BI-RADS 0, 1, or 2. For all malignant lesions, the percentage of cases assessed as BI-RADS 4–5 was almost perfect by ABUS and HHUS (99.13% and 99.42%), slightly better than that of MG (95.53%). The number of lesions assessed as BI-RADS 4 was 42 in MG, 2 in ABUS, and 3 in HHUS.

The agreement between ABUS and HHUS for all lesions was 86.63% (kappa = 0.77, $P<0.001$). The cross-tabulated data are shown in Table 1. There were a total of 46 (13.37%) discrepancies in all lesions, among which 34 lesions (73.91%) were assessed with a higher BI-RADS category by ABUS than by HHUS (Figure 1). The agreement between ABUS and MG was 32.22% (kappa = 0.10) for mammography-positive (BI-RADS 3, 4, and 5) cases. The cases assigned to the higher BI-RADS category by ABUS than by MG comprised 53.20% (183/344). The cross-tabulated data are presented in Table 2.

Lesion Size

Specific size measurements were obtained for all 344 lesions using ABUS and HHUS. The findings of MG were "nothing abnormal" in 2 cases, "breast hyperplasia" in 4 cases, "suspicious calcification" in 8 cases and "structural distortion" in 4 cases. As a result, 326 cases were measured by their specific size using MG.

Mean lesion sizes in the cases of breast cancer detected with the ABUS, HHUS, and MG were 23.2 ± 9.5 mm, 22.3 ± 6.3 mm, and 23.8 ± 12.0 mm, respectively, compared with the 19.9 mm (range: 5–70 mm) measured on histopathology. When we selected 3 mm as the threshold

for mis-sizing, lesion size was assessed correctly (± 3 mm) in 36.92% of the cases (N = 127) based on ABUS, 33.14% of the cases (N = 114) based on HHUS, and 33.44% of the cases (N = 109) based on MG. When we transformed the mis-sizing threshold from 3 mm to 5 mm, correct prediction (± 5 mm) was observed in 52.91% (N = 182) of ABUS, 48.84% (N = 168) of HHUS, and 43.87% (N = 143) of MG (Table 3). In our study group, all three imaging technologies showed a tendency to overestimate the malignant tumors: 40.99% and 32.85% with a threshold of 3 mm and 5 mm, respectively, in ABUS; 39.24% and 34.59% with a threshold of 3 mm and 5 mm, respectively, in HHUS; and 39.57% and 36.50% with a threshold of 3 mm and 5 mm, respectively, in MG.

With respect to the four major molecular subtypes, the lesion size on imaging and pathology was evaluated. Mean lesion sizes determined on histopathologic analysis were 18.2 mm, 20.2 mm, 23.9 mm, and 23.2 mm for luminal A subtype, luminal B, triple-negative, and HER2-enriched subtypes, respectively, compared with 21.4 mm, 23.3 mm, 26.4 mm, and 29.1 mm by ABUS, 19.9 mm, 23.4 mm, 27.6 mm, and 26.0 mm by HHUS, and 21.2 mm, 24.1 mm, 30.6 mm, and 29.5 mm by MG.

Coefficients of Correlation Between the Three Imaging Methods and Histopathology on Size Measurement

The overall correlation coefficients between predicted lesion size by imaging and histopathologic size were 0.75 Spearman for ABUS, 0.74 Spearman for HHUS, and 0.58 Spearman for MG. Both ABUS and HHUS results, but not MG results, were significantly correlated with the actual tumor size. The relationship between each imaging technique (ABUS, HHUS, and MG) and histopathology results is illustrated in Figure 2. In the comparison of malignant lesion assessments made with ABUS, HHUS, and MG, the correlation coefficients for the ABUS assessment were increased and independent of molecular subtypes. The correlation coefficients between ABUS and pathology were statistically higher than those between MG and pathology (P < 0.01), but not different from that between HHUS and pathology (P > 0.05).

Regarding the four major molecular subtypes, the correlation coefficient values between size on imaging and pathology were also evaluated. The average tumor size of each molecular type assessed by the three imaging methods and the correlation coefficient values between the sizes

Table 1 Cross-Tabulation of the BI-RADS Category in ABUS Vs HHUS

BI-RADS in ABUS	BI-RADS in HHHUS					
	3	4a	4b	4c	5	Total
3	1	2	0	0	0	3
4a	0	18	3	1	0	22
4b	0	6	50	2	0	58
4c	1	3	17	193	4	218
5	0	0	1	6	36	43
Total	2	29	71	202	40	344

Abbreviations: ABUS, automated breast ultrasound; HHUS, handheld ultrasound.
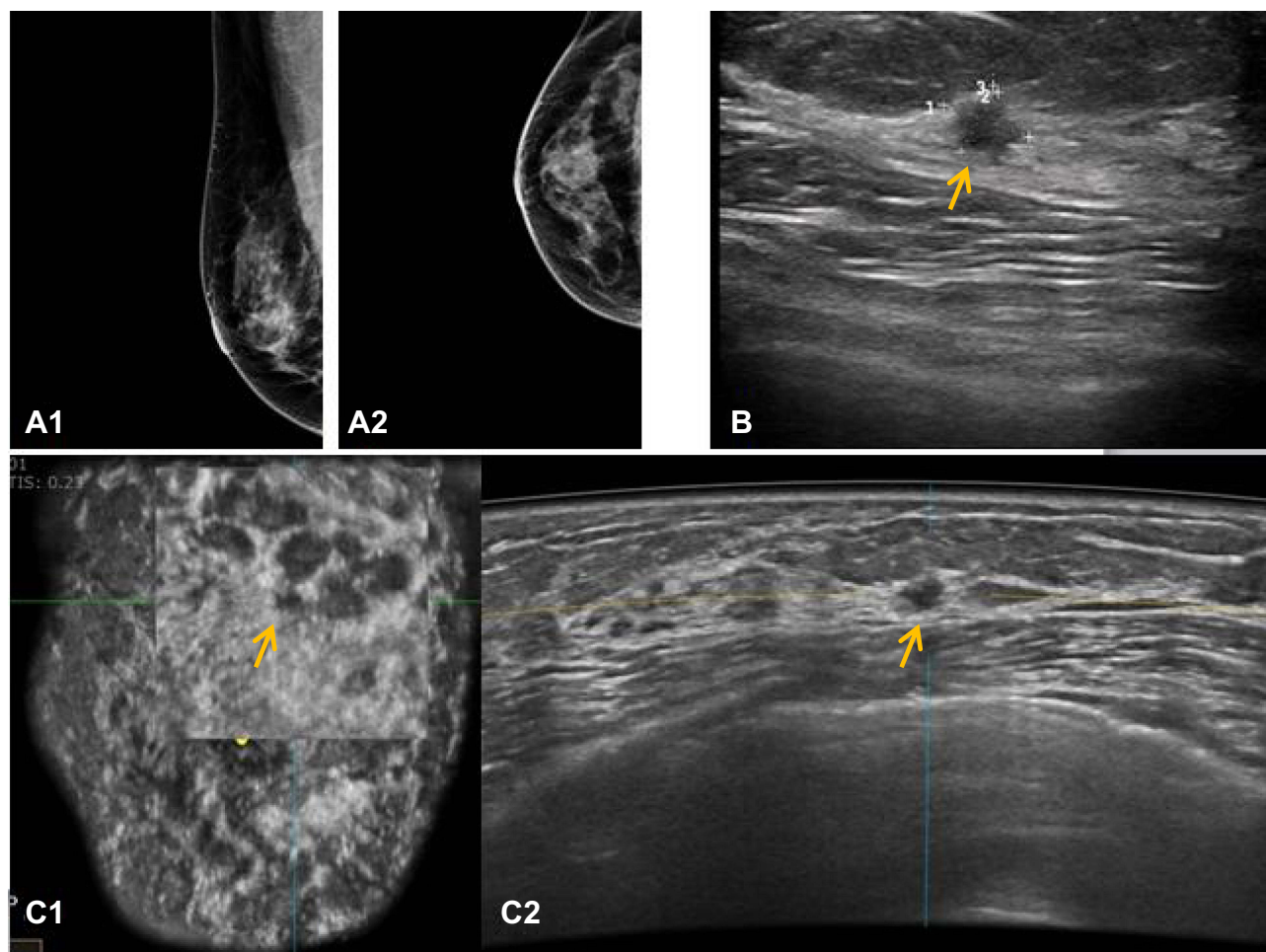
Figure 1 Fifty-one-year-old woman with invasive ductal carcinoma on the right breast. Final pathologic lesion size was 5mm. (**A1**) Mediolateral and (**A2**) craniocaudal mammography (MG) was negative. (**B**) Handheld breast ultrasound imaging (HHUS) showed a subtle irregular, angular, heterogeneous lesion in the upper quadrant, which was assessed as BI-RADS category 4A. Lesion size was measured as 7mm by HHUS. (**C2**) Automated breast ultrasound image (ABUS) revealed a relatively more prominent irregular, hypoechoic mass in the same location, the coronal-plane ABUS image (**C1**) well shows the spiculated and angled margin of the mass, which was assessed as BI-RADS category 4B. Lesion size was measured as 6mm by ABUS.

on the three imaging methods and pathology are shown in Table 4. The correlation coefficients between ABUS and pathology were statistically different from those between MG and pathology in the triple-negative, luminal B, and

Table 2 Cross-Tabulation of the BI-RADS Category in ABUS vs MG

BI-RADS in ABUS	BI-RADS in MG								
	0	1	2	3	4a	4b	4c	5	Total
3	0	1	0	1	1	0	0	0	3
4a	0	0	2	2	8	7	1	2	22
4b	0	1	2	9	21	15	8	2	58
4c	2	2	4	16	29	77	68	20	218
5	0	0	0	0	9	5	15	14	43
Total	2	4	8	28	68	104	92	38	344

Abbreviation: MG, mammography.

luminal A subtypes (P <0.01); the HER2-enriched subtype (P > 0.05) appears to be an exception. With ABUS, the size correlation coefficients of the triple-negative subtype (0.83, Spearman) were slightly higher than those of the luminal B (0.78, Spearman), luminal A (0.71, Spearman), and HER2-enriched subtypes (0.69, Spearman).

Discussion

Research on ABUS has been a hot spot in recent years. Yun et al, in a study performed on 135 asymptomatic women, noted that the agreement in confirmed malignancies was 55.1% (kappa = 0.39, $P<0.001$).[15] In our study group, the agreement on the BI-RADS category between ABUS and HHUS for confirmed malignant breast tumors was good (86.63%, kappa = 0.77). Among the discrepancies in all malignant cases, the BI-

Table 3 Assessment of the Size of Malignant Lesions Using the ABUS, HHUS and MG with Different Threshold

	With Threshold of 3 mm	With Threshold of 5 mm
ABUS(n = 344)		
Accurate estimation	127(36.92%)	182(52.91%)
Overestimations	141(40.99%)	113(32.85%)
Underestimation	76(22.09%)	49(14.24%)
HHUS(n = 344)		
Accurate estimation	114(33.14%)	168(48.84%)
Overestimations	135(39.24%)	119(34.59%)
Underestimation	98(27.62%)	57(16.57%)
MG(n = 326)		
Accurate estimation	109(33.44%)	143(43.87%)
Overestimations	129(39.57%)	119(36.50%)
Underestimation	87(26.69%)	64(19.63%)

RADS assessment category assigned using ABUS tended to be higher than HHUS. The interpretation of malignant lesions on both types of examination may be influenced by changes in the surrounding tissue and mass size.[16–18] The additional benefits of ABUS being able to perform on the coronal plane might contribute to such results. Image features such as the "retraction phenomenon sign," cord-like hyperechoic, angulation, and spiculated margins that are easily displayed on the coronal surface are usually available to predict malignant tumors. Vourtsis et al also suggested that an architectural distortion performed in the coronal plane was the only indication of the presence of an invasive lobular carcinoma.[19]

Additionally, it is reported that the agreement rate and kappa value between the ABUS and MG were 89.2% and 0.735, respectively.[20] However, our study results were unsatisfactory, with poor agreement (32.22%, kappa = 0.10) for mammography-positive (BI-RADS 3, 4, and 5) cases between MG and ABUS. Interestingly, the majority of the discordant cases involved a substantially lower grading of the BI-RADS category by MG than by ABUS. A potential reason might be that all the participants in our study were Chinese women who tended to have heterogeneously or extremely dense breasts. High breast density is an important factor in reducing the diagnostic capability of MG. Additionally, all lesions in the study were confirmed to be malignant by intraoperative pathology. Microlobulated margins and spiculated margins that tend to manifest in malignant tumors may be obscured in the background of dense

breast tissue. These elements may be responsible for the BI-RADS category of MG.

Regarding lesion size measurement between ABUS and HHUS, previous studies indicated that ABUS results were significantly more accurate in breast lesions. In a study with MRI serving as the gold standard, it was reported that the correlation of size measurement using automated breast volume scanning (ABVS)-MRI (r = 0.89) was slightly higher than that of HHUS-MRI (r = 0.82).[7] Li et al investigated 33 breast lesions (ductal carcinoma in situ), and the results suggested that the correlation coefficients between ABVS and histopathology results were very strong (0.720, Spearman), which is higher than that between histopathologic and HHUS measurements (0.371, Spearman).[21] In addition to the comparison of ABUS and HHUS, a comparison between MG and ABUS was also performed. In our investigation, both ABUS (0.75, Spearman) and HHUS (0.74, Spearman) results were significantly correlated with the actual tumor size when compared with the results of MG. The correlation coefficients between ABUS and pathology were statistically different from those between MG and pathology ($P<0.01$), but not different from that between HHUS and pathology ($P > 0.05$).

Regardless of whether 3 mm or 5 mm was chosen as the threshold, the accurate estimation was the highest on ABUS. We hypothesized that the features of breast volume images may be closely related to the satisfactory outcome between ABUS and histopathology-confirmed results. The coronal plane is one of its most obvious advantages. Just as surgeons viewed patients lying on the operating table, we were able to read the breast displayed in the same orientation. The coronal plane view, or the "surgical view," provides more understandable information on the extent of the breast's global visualization of anatomy and architecture. This may help distinguish between real solid lesions and inhomogeneous areas caused by hyperplastic breast tissue. This characteristic is advantageous for accurate measurement of breast lesions and offers more precise preoperative information for surgical plan interventions. More precise size information may be more helpful for TNM clinical grading of tumor. It may be used to determine the appropriate surgical margin for eligible breast-conserving surgery.

With respect to ABUS measurements in the four major molecular subtypes, the outcome of malignant tumor size measurements of the triple-negative subtype may be slightly better than those of the other subtypes, and those of the HER2-enriched subtype were at the bottom in this study. Similarly, Li et al reported that the triple-
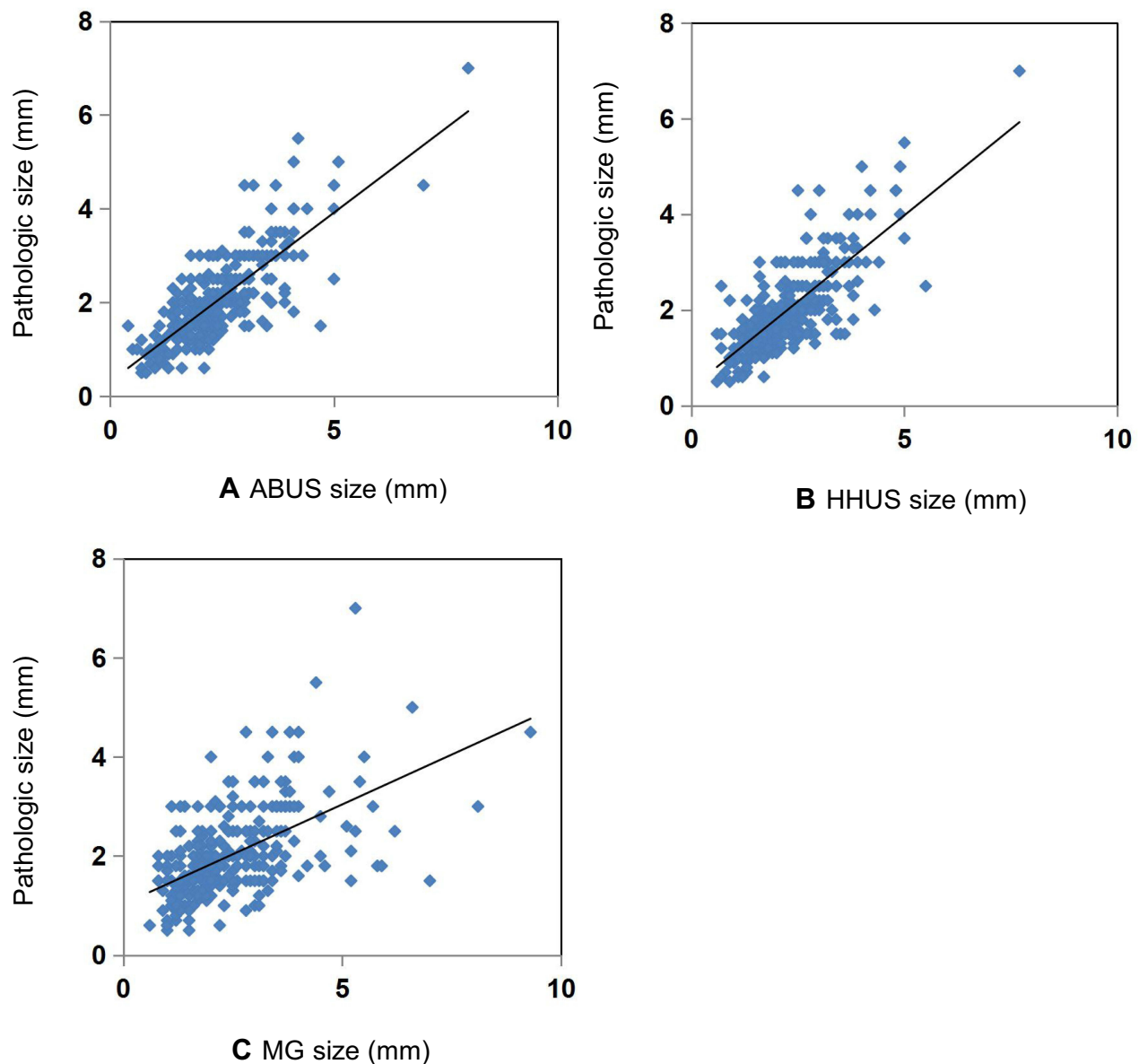
Figure 2 (**A**) Correlation of lesion size measured by automated breast ultrasonography (ABUS) and pathologic size. (**B**) Correlation of lesion size measured by handheld ultrasonography (HHUS) and pathologic size. (**C**) Correlation of lesion size measured by mammography (MG) and pathologic size.

negative subtype showed almost perfect reliability in the prediction of tumor size on ABUS by comparing four different imaging technologies.[22] We hypothesized that our results were related to the imaging performance of the molecular subtypes. Several previous studies have shown that the triple-negative subtype is more likely to perform as post-acoustic enhancement, regular shape, and microlobulated margins.[23–25] Imaging features that are almost similar to benign features can be attributed to the excellent outcome of triple-negative subtype size measurement. A study of 708 patients reported by Xu et al noted that structural deformation in the surrounding

tissues is often present in HER2+.[26] The fuzzy boundary caused by the higher degree of tumor invasion in HER2-enriched subtypes may not be as effective as the other three subtypes.

In this study, ABUS yielded results comparable to that of HHUS and, in some instances, even proved to be superior in malignant lesion size. Compared with HHUS, the other key advantages of ABUS are standardization, reproducible breast imaging, and the ability to analyze multiple images separately on a dedicated workstation according to our needs, which helps us improve reading efficiency. In a previous study, Van Zelst et al reported

Table 4 Malignant Tumor Size and Coefficients of Correlation Between Imaging and Histopathologic Results

| | Molecular Subtypes | | | | |
	Luminal A (N = 166)	Luminal B (N = 116)	Triple Negative (N = 30)	HER2 Enriched (N = 32)	Overall (N = 344)
ABUS					
Size	2.14	2.33	2.64	2.91	2.32
C	0.71	0.78	0.83	0.69	0.75
P	<0.01	<0.01	<0.01	<0.01	<0.01
HHUS					
Size	1.99	2.34	2.763	2.6	2.23
C	0.71	0.77	0.67	0.66	0.74
P	<0.01	<0.01	<0.01	<0.01	<0.01
MG					
Size	2.12	2.41	3.062	2.954	2.38
C	0.52	0.58	0.59	0.48	0.58
P	<0.01	<0.01	<0.01	0.007	<0.01
N missing	7	9	1	1	18

Abbreviation: C, Spearman correlation coefficient.

that the radiologists' diagnostic approach was facilitated by the implementation of multiplayer reconstruction data.[27] Approximately 3.5 min was needed for image interpretation per examination during our study, allowing a prevalent integration of ABUS into clinical implementation similar to the time reported by Somoinsight and less than the time reported in the EASY study.[10,11] In all related studies, it is important to note that the interpretation time was much less than the time required by the HHUS. Much information, including the lesion location based on the clock face location and the distance between the nipple and the skin, was displayed automatically by ABUS, allowing an objective and reliable record of the lesion and access to evaluate the image data for periodic checkups.

Our study suggested that MG was not comparable to ABUS in terms of the assessment of size measurement for breast cancer. Nevertheless, the superiority of MG in detecting microcalcifications has not been ignored. In our observation, the correlation coefficient between ABUS and histopathology was statistically better than MG and histopathology in the triple-negative subtype, luminal B subtype, and luminal A subtype ($P<0.05$), whereas the result for the HER2-enriched subtype was an exception with P > 0.05. Zheng et al suggested that calcifications are predictive factors of the HER2-enriched subtype.[28] Therefore, we believe that calcifications tending to be performed on HER2-enriched subtype

promote non-statistically different results between ABUS and MG. Finding a way to improve the ability to detect microcalcifications may be a promising approach for ABUS development.

Our study has several limitations. First, owing to the choice of study subjects, which were confirmed as malignant tumors, we could not provide some vital diagnostic abilities of ABUS, HHUS, and MG, such as sensitivity, specificity, positive predictive value, and negative predictive value. Second, this study was a retrospective investigation with a small sample and might only represented part of the general population, further prospective studies are needed to enrich the present findings. Third, our study was a single-factor analysis.

Conclusions

The BI-RADS category showed good agreement between ABUS and HHUS in cases of malignant breast lesions. ABUS may serve as an effective tool for evaluating tumor extent in breast cancer with a degree of accuracy similar to HHUS and greater than MG. As a promising imaging modality, ABUS is worthy of evaluation in larger prospective studies.

Ethics Approval and Informed Consent

The study was conducted in accordance with the Declaration of Helsinki (as was revised in 2013). This study was approved by the Ethics Committee of Harbin

Medical University Cancer Hospital. The requirement for informed patient consent was waived.

Consent for Publication

The authors confirm that the details of any images, videos and recordings can be published. All the authors listed have approved the manuscript for publication.

Author Contributions

All authors made substantial contributions to conception and design, acquisition of data, or analysis and interpretation of data; took part in drafting the article or revising it critically for important intellectual content; agreed to submit to the current journal; gave final approval for the version to be published; and agreed to be accountable for all aspects of the work.

Disclosure

The authors report no conflicts of interest in this work.

References

1. Sung H, Ferlay J, Siegel RL, et al. Global cancer statistics 2020: GLOBOCAN estimates of incidence and mortality worldwide for 36 cancers in 185 countries. *CA Cancer J Clin*. 2021;71(3):209–249. doi:10.3322/caac.21660
2. Shapiro S, Venet W, Strax P, Venet L, Roeser R. Ten- to fourteen-year effect of screening on breast cancer mortality. *J Natl Cancer Inst*. 1982;69(2):349–355.
3. Zhang Z, Wang W, Wang X, et al. Breast-specific gamma imaging or ultrasonography as adjunct imaging diagnostics in women with mammographically dense breasts. *Eur Radiol*. 2020;30(11):6062–6071. doi:10.1007/s00330-020-06950-2
4. Hooley RJ, Greenberg KL, Stackhouse RM, Geisel JL, Butler RS, Philpotts LE. Screening US in patients with mammographically dense breasts: initial experience with Connecticut Public Act 09-41. *Radiology*. 2012;265(1):59–69. doi:10.1148/radiol.12120621
5. Bae MS, Moon WK, Chang JM, et al. Breast cancer detected with screening US: reasons for nondetection at mammography. *Radiology*. 2014;270(2):369–377. doi:10.1148/radiol.13130724
6. Cho N, Han W, Han BK, et al. Breast cancer screening with mammography plus ultrasonography or magnetic resonance imaging in women 50 years or younger at diagnosis and treated with breast conservation therapy. *JAMA Oncol*. 2017;3(11):1495–1502. doi:10.1001/jamaoncol.2017.1256

7. Schmachtenberg C, Fischer T, Hamm B, Bick U. Diagnostic performance of automated breast volume scanning (ABVS) compared to handheld ultrasonography with breast MRI as the gold standard. *Acad Radiol*. 2017;24(8):954–961. doi:10.1016/j.acra.2017.01.021
8. Berg WA. Tailored supplemental screening for breast cancer: what now and what next. *AJR Am J Roentgenol*. 2009;192(2):390–399. doi:10.2214/AJR.08.1706
9. Chang JM, Cha JH, Park JS, Kim SJ, Moon WK. Automated breast ultrasound system (ABUS): reproducibility of mass localization, size measurement, and category on serial examinations. *Acta Radiol*. 2015;56(10):1163–1170. doi:10.1177/0284185114551565
10. Wilczek B, Wilczek HE, Rasouliyan L, Leifland K. Adding 3D automated breast ultrasound to mammography screening in women with heterogeneously and extremely dense breasts: report from a hospital-based, high-volume, single-center breast cancer screening program. *Eur J Radiol*. 2016;85(9):1554–1563. doi:10.1016/j.ejrad.2016.06.004
11. Brem RF, Tabár L, Duffy SW, et al. Assessing improvement in detection of breast cancer with three-dimensional automated breast US in women with dense breast tissue: the SomoInsight Study. *Radiology*. 2015;274(3):663–673. doi:10.1148/radiol.14132832
12. Silverstein MJ. The University of Southern California/Van Nuys prognostic index for ductal carcinoma in situ of the breast. *Am J Surg*. 2003;186(4):337–343. doi:10.1016/S0002-9610(03)00265-4
13. Sedgwick EL, Ebuoma L, Hamame A, et al. BI-RADS update for breast cancer caregivers. *Breast Cancer Res Treat*. 2015;150 (2):243–254. doi:10.1007/s10549-015-3332-4
14. Goldhirsch A, Winer EP, Coates AS, et al. Personalizing the treatment of women with early breast cancer: highlights of the St Gallen International Expert Consensus on the Primary Therapy of Early Breast Cancer 2013. *Ann Oncol*. 2013;24(9):2206–2223. doi:10.1093/annonc/mdt303
15. Yun G, Kim SM, Yun B, Ahn HS, Jang M. Reliability of automated versus handheld breast ultrasound examinations of suspicious breast masses. *Ultrasonography*. 2019;38(3):264–271. doi:10.14366/usg.18055
16. Choi EJ, Choi H, Park EH, Song JS, Youk JH. Evaluation of an automated breast volume scanner according to the fifth edition of BI-RADS for breast ultrasound compared with hand-held ultrasound. *Eur J Radiol*. 2018;99:138–145. doi:10.1016/j.ejrad.2018.01.002
17. Jeh SK, Kim SH, Choi JJ, et al. Comparison of automated breast ultrasonography to handheld ultrasonography in detecting and diagnosing breast lesions. *Acta Radiol*. 2016;57(2):162–169. doi:10.1177/0284185115574872
18. Chang JM, Moon WK, Cho N, Park JS, Kim SJ. Breast cancers initially detected by hand-held ultrasound: detection performance of radiologists using automated breast ultrasound data. *Acta Radiol*. 2011;52(1):8–14. doi:10.1258/ar.2010.100179
19. Vourtsis A, Kachulis A. The performance of 3D ABUS versus HHUS in the visualisation and BI-RADS characterisation of breast lesions in a large cohort of 1886 women. *Eur Radiol*. 2018;28(2):592–601. doi:10.1007/s00330-017-5011-9
20. Zhang X, Lin X, Tan Y, et al. A multicenter hospital-based diagnosis study of automated breast ultrasound system in detecting breast cancer among Chinese women. *Chin J Cancer Res*. 2018;30 (2):231–239. doi:10.21147/j.issn.1000-9604.2018.02.06
21. Li N, Jiang YX, Zhu QL, et al. Accuracy of an automated breast volume ultrasound system for assessment of the pre-operative extent of pure ductal carcinoma in situ: comparison with a conventional handheld ultrasound examination. *Ultrasound Med Biol*. 2013;39 (12):2255–2263. doi:10.1016/j.ultrasmedbio.2013.07.010
22. Park J, Chae EY, Cha JH, et al. Comparison of mammography, digital breast tomosynthesis, automated breast ultrasound, magnetic resonance imaging in evaluation of residual tumor after neoadjuvant chemotherapy. *Eur J Radiol*. 2018;108:261–268. doi:10.1016/j.ejrad.2018.09.032

23. Boisserie-Lacroix M, Macgrogan G, Debled M, et al. Triple-negative breast cancers: associations between imaging and pathological findings for triple-negative tumors compared with hormone receptor-positive/human epidermal growth factor receptor-2-negative breast cancers. *Oncologist*. 2013;18(7):802–811. doi:10.1634/theoncologist.2013-0380

24. Yang Q, Liu HY, Liu D, Song YQ. Ultrasonographic features of triple-negative breast cancer: a comparison with other breast cancer subtypes. *Asian Pac J Cancer Prev*. 2015;16(8):3229–3232. doi:10.7314/APJCP.2015.16.8.3229

25. Zheng FY, Yan LX, Huang BJ, et al. Comparison of retraction phenomenon and BI-RADS-US descriptors in differentiating benign and malignant breast masses using an automated breast volume scanner. *Eur J Radiol*. 2015;84(11):2123–2129. doi:10.1016/j.ejrad.2015.07.028

26. Xu J, Ma G, Liang M, et al. Factors that influence ultrasound evaluation of breast tumor size. *Med Ultrason*. 2019;21(2):144–151. doi:10.11152/mu-1747

27. Van Zelst JC, Platel B, Karssemeijer N, Mann RM. Multiplanar reconstructions of 3D automated breast ultrasound improve lesion differentiation by radiologists. *Acad Radiol*. 2015;22(12):1489–1496. doi:10.1016/j.acra.2015.08.006

28. Zheng FY, Lu Q, Huang BJ, et al. Imaging features of automated breast volume scanner: correlation with molecular subtypes of breast cancer. *Eur J Radiol*. 2017;86:267–275. doi:10.1016/j.ejrad.2016.11.032